Desalination and Water Treatment
www.deswater.com

doi: 10.1080/19443994.2014.981866

57 (2016) 2064–2072
January

Taylor & Francis
Taylor & Francis Group

Removal of Cu^{2+} from the aqueous solution by tartrate-intercalated layered double hydroxide

Yanming Shen*, Xiaolei Zhao, Xi Zhang, Shifeng Li, Dongbin Liu, Lihui Fan

Department of Chemical Engineering, Shenyang University of Chemical Technology, No. 11 Street, Shenyang Economical and Development Zone, Shenyang 110142, Liaoning, P.R. China, Tel. +86 24 89383529; Fax: +86 24 89383760;
emails: sym6821@sina.com.cn (Y. Shen), 531476731@qq.com (X. Zhao), 504844801@qq.com (X. Zhang), li.shi.feng@163.com (S. LI), liudongbin@139.com (D. Liu), flh8947@163.com (L. Fan)

Received 25 April 2014; Accepted 24 October 2014

ABSTRACT

The tartrate-intercalated MgAl layered double hydroxide (MgAl-TA LDH) was prepared by ion-exchange method at the acid solution using MgAl-CO_3 LDH as the precursor. The adsorption of Cu^{2+} on MgAl-TA LDH was studied and some influence factors such as contact time, initial Cu^{2+} concentration, adsorbent dosage, solution pH, and adsorption temperature were investigated. Three kinds of adsorption isotherms (Langmuir model, Freundlich model, and Redlich–Peterson model) were investigated; the results indicated that equilibrium was well described by Langmuir isotherm, predicting the adsorption of Cu^{2+} on MgAl-TA adsorbents was a monolayer adsorption. The equilibrium kinetic adsorption data were fitted to the pseudo-second order kinetic equation. Furthermore, the adsorption of Cu^{2+} was controlled mainly by chemical process combined with intra-particle diffusion. Parameters of adsorption thermodynamic suggested that the interaction of Cu^{2+} adsorbed by MgAl-TA LDH adsorbents was spontaneous and endothermic.

Keywords: Layered double hydroxide; Hydrotalcite; Adsorption; Heavy metal ion; Regeneration

1. Introduction

With the rapid development of industries, such as metal plating facilities, mining operations, fertilizer industries, tanneries, batteries, paper industries, and pesticides, heavy metals wastewaters are directly or indirectly discharged into the environment increasingly, especially in developing countries. Unlike organic contaminants, heavy metals are not biodegradable and tend to accumulate in living organisms and many heavy metal ions that are known to be toxic or carcinogenic [1]. Various physical–chemical processes have been extensively used in the treatment of heavy metal wastewater, including chemical precipitation, ion-exchange, and electrochemical treatment [2]. Among these methods, adsorption is now recognized as an effective and economic method for the heavy metal wastewater treatment. The adsorption process offers flexibility in design and operation and in many cases will produce high-quality treated effluent. In addition, because adsorption is sometimes reversible, adsorbents can be regenerated by suitable desorption process [3]. Besides the common activated carbon adsorbents, many low-cost adsorbents such as

*Corresponding author.

agricultural wastes [4,5], industrial by-products and wastes [6] and natural substances [7] have been studied as adsorbents for the heavy metal wastewater treatment. Recently, layered double hydroxides (LDH) were developed as the adsorbents to adsorb heavy metal ions from wastewater owing to their layer structure, good anion-exchange capacity, simple synthesis, low cost and environmental friendliness [8,9]. It was reported that Pb^{2+} and Cu^{2+} could be uptaken rapidly from an aqueous solution on Mg–Al LDHs mainly by surface complex adsorption and precipitation [10,11]. It was also found that high affinity and large removal capacity of Cu^{2+}, Cd^{2+}, and Pb^{2+} were obtained on Ca-Al-NO_3 LDHs via a hydroxide precipitation mechanism [12].

The chelating agents are often used in the remediation of metal-contaminated soils by phytoextraction in order to increase metal mobility and enhance its uptake by plants [13]. Thus, some researchers attempted to introduce the chelating agents into the interlayer space of LDH to improve the adsorption capacity for heavy metal ions. Ethylenediaminetetraacetic acid (EDTA) is probably the most efficient chelating agent for enhancing metal uptake by plants. Kameda et al. found that EDTA anion-intercalated Mg–Al LDH (EDTA·Mg–Al LDH) rapidly and selectively took up heavy metal ions such as Cu^{2+} and Cd^{2+} from aqueous solutions [14], which was attributable to the formation of an EDTA–metal complex in the interlayer of Mg–Al LDH. Perez et al. also examined the uptake of Cu^{2+}, Cd^{2+}, and Pb^{2+} by Zn–Al LDH intercalated with EDTA [15]. However, the lower degradation of EDTA increase the risk of pollution. Organic acids such as citric, malic, and tartaric acids were also found to be effective for the leaching of heavy metals due to the formation of chelate complexes between the metals and acids [16]. Tartaric acid (TA), a carboxylic acid with mild chemical properties, inexpensive, and environmentally friendly, is naturally more abundant than EDTA and is therefore more suitable for large-scale remediation of aqueous environments [17,18].

In the present work, an easy and efficient method to intercalate the tartrate ion into the MgAl LDH was developed. The resultant new material was applied to the removal of Cu^{2+} from the aqueous solution, to evaluate its efficiency. The regeneration ability was also investigated for the potential application in practice.

2. Materials and methods

2.1. Adsorbent

2.1.1. Preparation of adsorbent

The carbonate-intercalated MgAl LDH precursor with Mg/Al ratio of 2.0 was prepared by co-precipitation as described elsewhere [19], and the resultant material was labeled as MgAl-CO_3 LDH. The tartrate-intercalated MgAl LDH was prepared by the anion-exchange method. Typically, 0.72 g disodium tartrate was dissolved in 100 ml ethylene glycol in a three-neck flask. The pH was adjusted in the range of 4–5 by adding 0.1 mol L^{-1} HNO_3. Then, 2.0 g as-prepared MgAl-CO_3 LDH was added into the above solution. The mixture was kept refluxing at 120°C for 5 h and then cooled to room temperature. The resultant solid was recovered by filtering the resultant suspension, which was followed by repeated washing with deionized water and drying at 80°C for 12 h. The resultant solid was labeled as tartrate intercalated MgAl layered double hydroxide (MgAl-TA LDH).

All the reagents were of analytical grade and purchased from Sinopharm Chemical Reagent Company, Ltd, China. They were used without further purification.

2.1.2. Characterization techniques

The phases of the resultant samples were analyzed by X-ray diffraction (XRD) using a Brucker D8 ADVANCE diffractometer under CuKα radiation ($\lambda = 0.15406$ nm), operating at 40 kV and 40 mA over 2θ range from 3 to 75. FT-IR spectra were recorded on Nicolet Nexus 470 spectrometer (Thermo Nicolet Corporation, USA) under scan range 400–4,000 cm^{-1} using KBr pellets (1/10 wt.%). Scanning electron microscope (SEM) images were taken by JSM-6360LV (JEOL, Japan) at 10.0 kV.

2.2. Adsorbate

Copper stock solution of 1,000 mg L^{-1} was prepared using $Cu(NO_3)\cdot 3H_2O$ of analytical reagent grade into deionized water. In this study, the initial Cu^{2+} concentration was varied from 10 to 200 mg L^{-1}.

2.3. Experimental process

2.3.1. Effect of adsorbent dosage

The effect of adsorbent dosage on the amount of Cu^{2+} adsorbed was obtained by agitating 100 mL of Cu^{2+} solution of initial Cu^{2+} concentration of 100 mg L^{-1} with weighed amount of MgAl-TA LDHs (1, 2, 4, and 5 g/L) till equilibrium reached at 25°C.

2.3.2. Effect of initial adsorbate concentration

The effect of initial adsorbate concentration on the amount of Cu^{2+} adsorbed was obtained by adding

2.0 g L^{-1} MgAl-TA LDHs into 100 mL of Cu^{2+} solution of initial Cu^{2+} concentration of a certain value (10, 30, 50, 80, 100, 150, and 200 mg L^{-1}) and then agitating the solution till equilibrium reached at 25°C.

2.3.3. Effect of pH

The batch adsorption studies were carried out at different pH values in the range of 3–10. The pH was adjusted using 0.1 mol L^{-1} NaOH and HNO_3 solutions. MgAl-TA LDHs were added to 100 mL solution with the dosage of 4 g L^{-1} while being agitated using 250 mL shaking flasks at 25°C for 24 h in each test.

2.3.4. Effect of adsorption temperature

The effect of adsorption temperature on the amount of Cu^{2+} adsorbed was carried out as follows: MgAl-TA LDHs with the dosage of 2 g L^{-1} were added to 100 mL solution Cu^{2+} solution with initial Cu^{2+} concentration of 100 mg L^{-1}, and then, the solution was agitated at a certain temperature (25, 30, and 40°C) till equilibrium reached.

2.3.5 Analysis methods

The concentration of Cu^{2+} was determined by atomic adsorption spectrophotometer (AA-6300C, Oxford, Japan). Metal ion removal capacities of the samples were calculated as follows:

$$\text{Removal efficiency } (\eta\%) = \frac{C_0 - C_t}{C_0} \times 100\% \quad (1)$$

$$q_t = \frac{(C_0 - C_t)V}{m} \quad (2)$$

where q_t, the amounts of Cu^{2+} adsorbed at adsorption time t (mg g^{-1}); C_0, the initial concentration of Cu^{2+} in the solution (mg L^{-1}); C_t, the concentration of Cu^{2+} in the solution at adsorption time t (mg L^{-1}); V, volume of the solution (L); and m, weight of the adsorbent (g).

2.3.6 Adsorbent regeneration

Firstly, the ammonium solution with concentration of 10 wt.% was prepared for regeneration solution. Then, the used MgAl-TA particles were added into the above solution at the dosage of 0.02 g ml^{-1} and kept regeneration for 1 h under stirring. After being filtrated, washed with deionized water, and dried at 80°C, the MgAl-CO_3 LDH precursor was obtained. The regenerated MgAl-TA LDH was prepared according to the steps described as Section 2.1.1.

3. Results and discussion

3.1. Characterization of MgAl-TA adsorbent

The powder XRD patterns of the precursor MgAl-CO_3 LDH and the resulting MgAl-TA are shown in Fig. 1. The XRD pattern of MgAl-CO_3 LDH (Fig. 1(a)) shows four characteristic peaks at 2θ = 11.6°, 23.4°, 35.1°, and 61.1° that are related to their corresponding indices (0 0 3), (0 0 6), (0 0 9), and (1 1 0), respectively (JCPDS 41-1428). The MgAl-CO_3 LDH precursor gives a basal spacing of 0.76 nm which is calculated from the (0 0 3) diffraction at $2\theta = 11.6°$. The interlayer spacing is 0.28 nm by subtracting the thickness of the brucite-like layers (0.48 nm) from the basal spacing. As shown in Fig. 1(b), MgAl-TA LDH shows obvious shift in the (0 0 3) reflection to lower angle, indicating that the TA anions have been successfully intercalated into the interlayer region. By contrast, the reflection lines of the diffraction peak (ambient 61.1°) do not move, which indicates that the intercalation of the TA does not change the structure of the layer but only changes the interlayer spacing [20]. The basal spacing expands to 1.22 nm, when CO_3^{2-} is replaced by TA in an ion-exchange reaction.

The SEM image of MgAl-TA shown in Fig. 2 indicates the plate-like structure and the plate-like slabs stack closely with each other, which is typical for LDH.

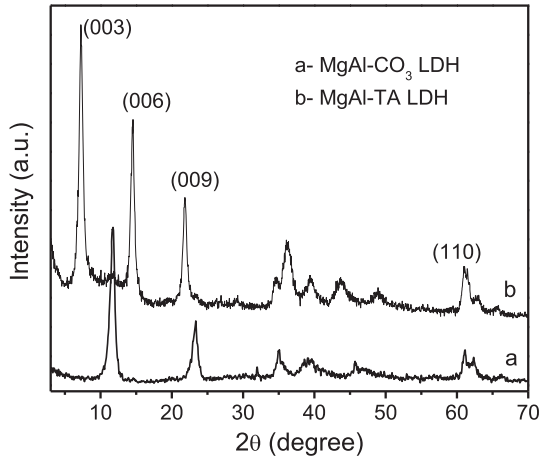

Fig. 1. XRD patterns of MgAl-CO_3 LDH (a) and MgAl-TA LDH (b).

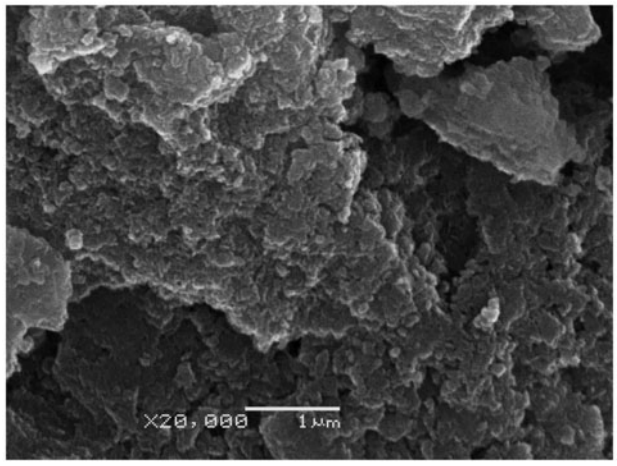

Fig. 2. SEM image of MgAl-TA LDH.

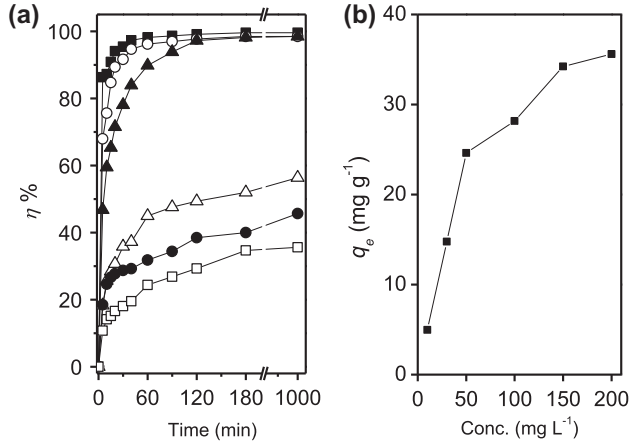

Fig. 4. The variations of η% (a) and q_e (b) with initial Cu^{2+} concentration. ■: 10, ○: 30, ▲: 50, △: 100, ●: 150, and □: 200 mg L^{-1}.

3.2. Effect of MgAl-TA adsorbent dosage

The effects of adsorbent dose on the removal efficiency (%) for the adsorbent are shown in Fig. 3. It can be found that the removal efficiency increases rapidly in the first 60 min, then reaches the equilibrium. It is also observed that removal efficiency increases, but the amount of Cu^{2+} adsorbed onto unit weight of adsorbent at equilibrium (q_e) decreases (see Fig. 3(b)), with the increase in the initial MgAl-TA adsorbent dosage. The increase in removal efficiency is due to the increase in the vacant adsorption sites with increasing adsorbent thus favoring more Cu^{2+} uptake, while the decrease in q_e may be due to the reduction in overall surface area of the sorbent probably because of aggregation during the adsorption [2].

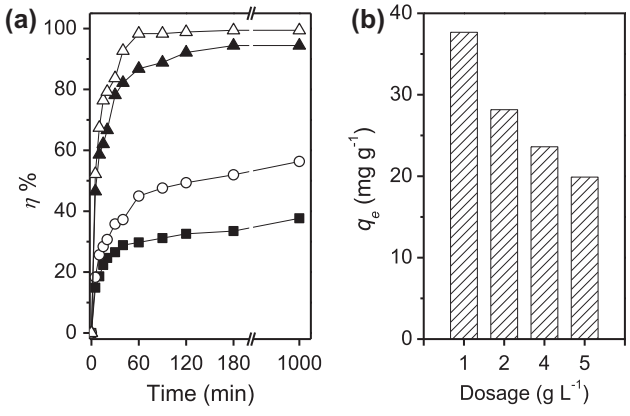

Fig. 3. The variations of η% (a) and q_e (b) with the MgAl-TA adsorbent dosage. ■: 1, ○: 2, ▲: 4, and △: 5 g L^{-1}.

3.3. Effect of initial Cu^{2+} concentration

Fig. 4 shows the effect of initial Cu^{2+} concentration on the removal efficiency. As shown in Fig. 4, the removal efficiency for Cu^{2+} decreases with the increase in initial Cu^{2+} concentration. However, the adsorbed amounts of Cu^{2+} per mass of adsorbent are higher in higher initial Cu^{2+} concentrations as compared to the lower initial Cu^{2+} concentrations (see Fig. 4(b)). The Cu^{2+} concentration provides an important driving force to overcome the mass transfer resistance between adsorbents and aqueous solutions. It means that at higher initial Cu^{2+} concentrations, the driving force was higher than that of the lower initial Cu^{2+} concentrations. Consequently, the adsorbed amounts of Cu^{2+} per mass of adsorbent will be higher in case of higher initial Cu^{2+} concentrations. However, at higher initial Cu^{2+} concentrations, the available adsorption sites becomes comparatively fewer and hence lowering the removal percentage of Cu^{2+}.

3.4. Effect of pH

The pH effect on Cu^{2+} adsorption onto MgAl-TA LDH adsorbent is shown in Fig. 5. It is seen that the removal efficiency is low at low pH values. It increases with the increase in the pH value and reaches the maximum at pH of 5.0–6.0 and then slightly decreased to a plateau at pH value above 7.0. The surface of MgAl-TA LDH contains a large number of binding sites and may become positively charged at low pH due to the protonation reaction on the surfaces (i.e. $SOH + H^+ \Leftrightarrow SOH_2^+$). At pH value under the zero charge point (ZCP), the surfaces are positively charged, and there exist appreciable concentrations of

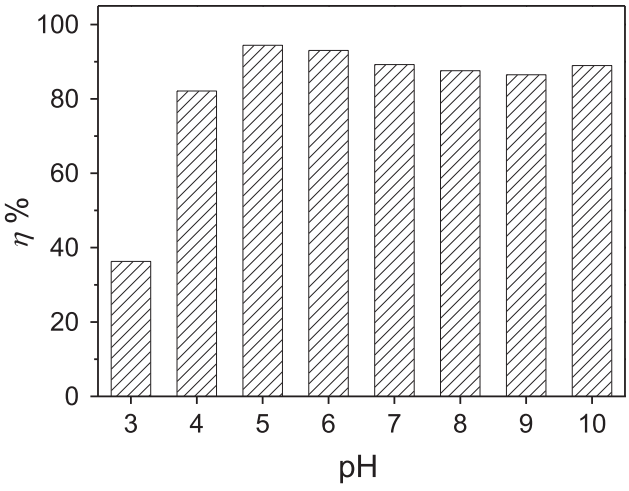

Fig. 5. The variations of η% with pH.

H^+ ions that compete with already present Cu^{2+} ions for available binding sites, resulting in the decrease in the copper uptake. At the pH value above the ZCP, the surfaces are negatively charged, the number of H^+ ions decreases and hence, more sites are available for copper uptake [2,10]. It should be noted that the pH of the initial adsorbate solution is about 5.0–6.0 itself, approaching the suitable pH for Cu^{2+} adsorption.

3.5. Effect of adsorption temperature

As shown in Fig. 6, it is observed that the removal efficiency increases by increasing the adsorption temperature from 25 to 40°C, showing that the adsorption process is endothermic. Moreover, the adsorption equilibrium can be rapidly reached at higher temperature.

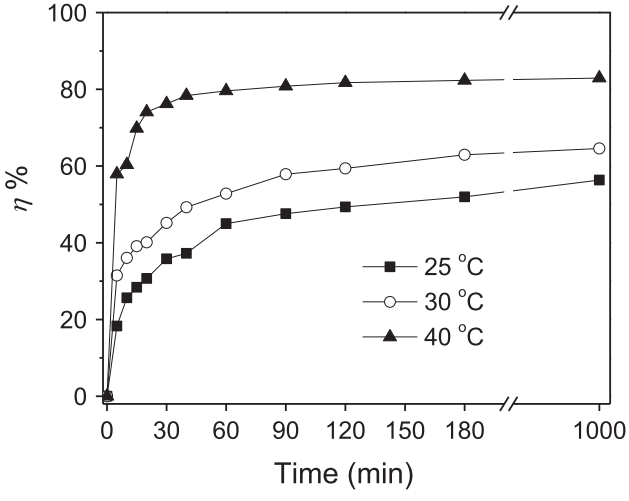

Fig. 6. The variations of η% with adsorption temperature.

3.6. Adsorption kinetics

In order to evaluate the adsorption kinetics of Cu^{2+} onto MgAl-EDTA LDH adsorbent, Lagergren pseudo-first-order, pseudo-second-order, intra-particle diffusion, and Elovich kinetics models were applied to fit the experimental data. These model expressions can be described as follows:

$$\text{First-order equation}: q_t = q_e(1 - e^{-k_1 t}) \quad (3)$$

$$\text{Second-order equation}: q_t = \frac{k_2 q_e^2 t}{1 + k_2 q_e t} \quad (4)$$

$$\text{Intra-particle diffusion equation}: q_t = k_3 t^{0.5} + C \quad (5)$$

$$\text{Elovich equation}: q_t = \beta \ln(\alpha\beta) + \beta \ln t \quad (6)$$

where q_e and q_t are the amounts of Cu^{2+} adsorbed at equilibrium and at time t (mg g^{-1}), respectively. k_1 (min^{-1}) and k_2 (g mg^{-1} min^{-1}) are the rate constants of first-order and second-order adsorption, respectively. The coefficient α is the initial adsorption rate [g (mg $min^2)^{-1}$] and β is the desorption constant [mg $(g\ min)^{-1}$] related to the extent of surface coverage and activation energy for chemisorption. The fitting curves are shown in Fig. 7, and the calculated kinetic parameters for pseudo-first-and pseudo-second-order models are listed in Table 1. The determination coefficients R^2 listed in Table 1 indicate that the experimental data are in good agreement with the pseudo-second order model, which suggests that the rate-limiting step in adsorption is controlled by chemical process [21].

The intra-particle diffusion equation describes the movement of ions from bulk solution to the solid phase. As shown in Fig. 7(c), the plots of q_t vs. $t^{1/2}$ for Cu^{2+} are shown in two stages. The first straight portion depicts macropore diffusion, and the second one represents micropore diffusion. The line of best fit within 60 min does not pass through the origin, which is a requirement if this model is to be obeyed. The strong linear correlation indicates that intra-particle diffusion is involved in the adsorption process, but the non-zero intercept suggests that it is not the rate-controlling step [22].

The Elovich equation interprets the predominantly chemical adsorption on highly heterogeneous adsorbents. As described in Fig. 7(d), the plots of q_t vs. ln (t) display relative good linear relationship before reaching the adsorption equilibrium. This result shows that the heterogeneous distribution of adsorption energy in adsorption process.

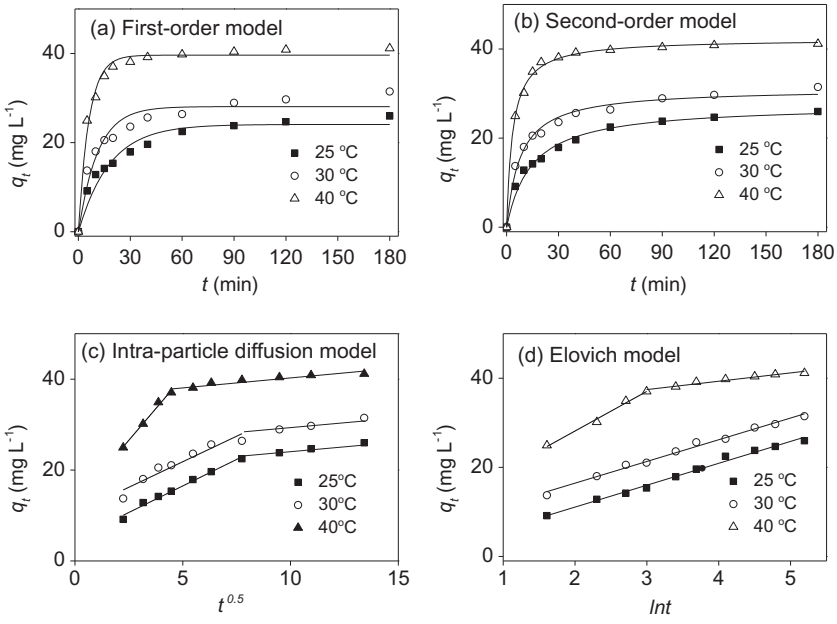

Fig. 7. Kinetics fitting curves for adsorption of Cu^{2+} at different temperatures.

Table 1
Parameters of adsorption kinetics

	Pseudo-first order			Pseudo-second order		
Temperature (°C)	q_{e1} (mg g^{-1})	K_1 (min^{-1})	R^2	q_{e2} (mg g^{-1})	K_2 (g mg^{-1} min^{-1})	R^2
25	23.91	0.0584	0.9470	27.06	0.00285	0.9866
30	28.09	0.0903	0.9346	31.12	0.00412	0.9857
40	39.64	0.1634	0.9849	42.20	0.00664	0.9976

3.7. Adsorption isotherm

An adsorption isotherm represents the amount of species adsorbed versus the amount of species left in the solution phase at equilibrium. The adsorption data were analyzed by Langmuir, Freundlich, and Redlich–Peterson isotherms, which can be described as following equations, respectively:

$$\text{Langmuir equation}: q_e = \frac{q_{\max} K_L C_e}{1 + K_L C_e} \quad (7)$$

$$\text{Freundlich equation}: q_e = K_F C_e^{\frac{1}{n}} \quad (8)$$

$$\text{Redlich–Peterson equation}: q_e = \frac{AC_e}{1 + BC_e^{\beta}} \quad (9)$$

where q_e is the amount of Cu^{2+} adsorbed on the adsorbent at equilibrium (mg g^{-1}), $q_{\max}$ denotes the maximum adsorption capacity corresponding to complete monolayer coverage, C_e describes the equilibrium Cu^{2+} concentration (mg L^{-1}), and K_L is the Langmuir adsorption constant (L mg^{-1}). While K_F and n are the Freundlich constants related to the maximum adsorption capacity (mg g^{-1}) and the heterogeneity factor (mg^{-1}), respectively. In Redlich–Peterson equation, A (L g^{-1}) and B (L mg^{-1})$^{\beta}$ are the Redlich–Peterson isotherm constants, while β is the Redlich–Peterson isotherm exponent. For $\beta = 1$, the Redlich–Peterson model converts to the Langmuir model. By non-linear fitting, the results were obtained and listed in Table 2. As shown in Table 2, both Langmuir and Redlich–Peterson isotherm model fit the experimental data better than Freundlich model. Fig. 8 shows the Langmuir fitting curves. In this work, the Redlich–Peterson isotherm exponents β is close to 1, showing the adsorption isotherm approaches to Langmuir model.

Table 2
Parameters of adsorption isotherms

Temperature (°C)	Langmuir				Freundlich		
	q_{max}	K_L	R^2	R_L	n	K_F	R^2
25	30.76	0.3493	0.9770	0.028–0.36	4.357	12.24	0.9035
30	36.67	0.5066	0.9851	0.019–0.28	4.412	15.41	0.8771
40	51.27	0.6690	0.9839	0.015–0.23	4.437	22.60	0.8344
Temperature (°C)	Redlich–Peterson						
	A	B	β	R^2			
25	12.22	0.4463	0.9709	0.9722			
30	20.17	0.5946	0.9791	0.9821			
40	29.78	0.5052	1.0039	0.9820			

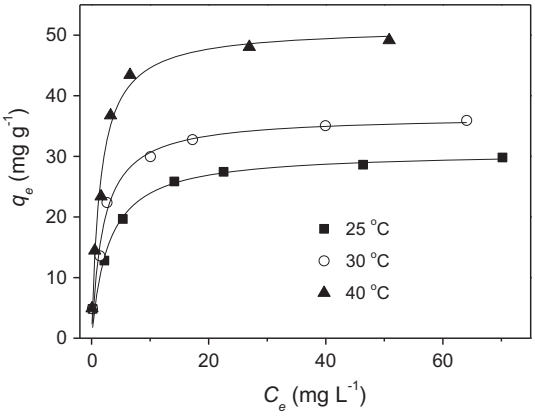

Fig. 8. Langmuir Isotherms of Cu^{2+} on MgAl-TA adsorbent at different temperatures.

The dimensionless constant called separation factor (R_L, also called equilibrium parameter) is commonly used to predict whether an adsorption system is favorable or unfavorable. The R_L is expressed as:

$$R_L = \frac{1}{1 + K_L C_0} \tag{10}$$

The value of R_L indicates the adsorption process to be irreversible ($R_L = 0$), favorable ($0 < R_L < 1$), linear ($R_L = 1$), or unfavorable ($R_L > 1$). The calculated results listed in Table 2 show the adsorption of Cu^{2+} onto MgAl-TA LDH is favorable [4]. The adsorption capacity calculated from Langmuir model is 30.76, 36.67, and 51.27 mg g^{-1} at temperature of 25, 30, and 40°C, respectively.

3.8. Adsorption thermodynamic

Thermodynamic parameters of adsorption of Cu^{2+} onto MgAl-TA adsorbent are evaluated using the following equations [23]:

$$\Delta G^0 = -RT \cdot \ln k_c \tag{11}$$

$$\Delta G^0 = \Delta H^0 - T\Delta S^0 \tag{12}$$

$$\ln k_c = \frac{\Delta S^0}{R} - \frac{\Delta H^0}{RT} \tag{13}$$

where R is the universal gas constant (8.314 J mol^{-1} K^{-1}), T is the temperature (K), ΔG^0 is the change in free energy, ΔH^0 is the standard enthalpy, and ΔS^0 is the standard entropy. Value of $\ln k_c$ can be obtained by plotting $\ln (q_e/C_e)$ vs. q_e for adsorption of Cu^{2+} onto MgAl-TA LDH and extrapolating q_e to zero [24]. The values are obtained as 3.99 ($T = 25$°C), 4.15 ($T = 30$°C), and 4.67 ($T = 40$°C). ΔH^0 and ΔS^0 can be calculated, respectively, from the slope and intercept of plot of $\ln k_c$ vs. $1/T$. The values obtained from Eqs. (11)–(13) are listed in Table 3.

As listed in Table 3, the positive value of the standard enthalpy change (ΔH^0) shows that the adsorption is endothermic, which follows the result observed from the effect of temperature on the removal efficiency. The reason may be explained that, at a higher temperature, an increase in active sites occurs owing to bond rupture of functional groups on adsorbent surface [2,10]. When the adsorption force is van der Waals force, the adsorption heat is 4–10 kJ mol^{-1}; when the force is a hydrogen-bonding force, the adsorption heat is 2–40 kJ mol^{-1}. As the force is the exchange of dentate, dipole−dipole interaction, and chemical bonds force, the adsorption heat is about 40 kJ mol^{-1}, 2–29 kJ mol^{-1}, and above 60 kJ mol^{-1}, respectively [25]. The value of ΔH^0 indicates that the adsorption force perhaps is hydrogen-bonding force. The negative value of ΔG^0 indicated the spontaneous nature of adsorption process, and it is more negative at higher temperature, which indicates that the

Table 3
Parameters of adsorption thermodynamics parameters

Temperature (°C)	ΔG^0 (kJ mol^{-1})	ΔH^0 (kJ mol^{-1})	ΔS^0 (J mol^{-1} K^{-1})	E_a (kJ mol^{-1})[a]
25	−9.89	35.93	0.153	42.93
30	−10.46			
40	−12.16			

[a]The activation energy E_a calculated according to the pseudo-second-order kinetics model.

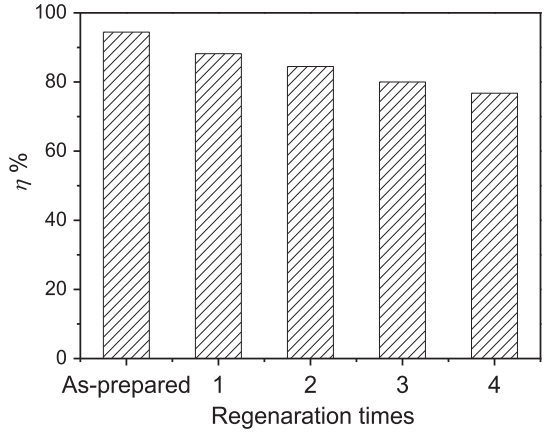

Fig. 9. Effect of regeneration times on the adsorption of Cu^{2+}. Adsorption condition: temperature of 25°C, adsorbent dosage of 4 g L^{-1}, and initial Cu^{2+} concentration of 100 mg L^{-1}.

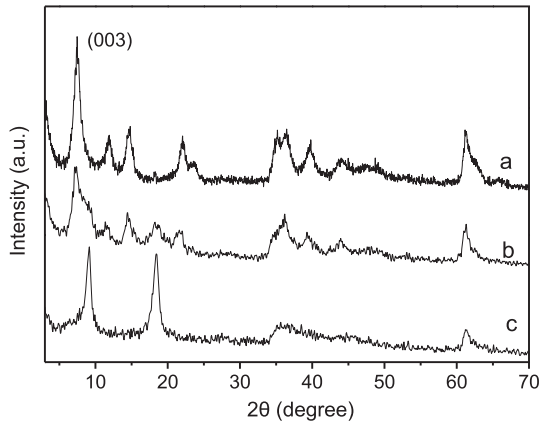

Fig. 10. XRD patterns of MgAl-TA LDH adsorbent before (a), after regeneration for one times (b), and four times (c).

spontaneity of the adsorption process increases with the rise in temperature. The positive value of entropy change (ΔS^0) implies some structural changes in adsorbate and adsorbent during the adsorption process, which leads to an increase in the disorderness of the solid-solution system. The activation energy E_a calculated according to the pseudo-second order kinetics model is 42.93 kJ mol^{-1}, suggesting that the adsorption process is belonged to chemical process [26].

3.9. Adsorbent regeneration

Effective reuse of adsorbent material directly affects the cost factor and hence its utility in continuous batch adsorption processes. In this work, the regeneration of the used MgAl-TA adsorbent was investigated. Firstly, the ammonium solution was used as extracting agent to extract Cu^{2+} from the adsorbent by forming $[Cu(NH_3)_4]^{2+}$, which is dissolved in water. After separation of the solid adsorbent from the solution, the solid was re-exchanged with TA solution, forming the MgAl-TA adsorbent. The left solution with higher concentration of Cu^{2+} can be further treatment, such as producing copper salts. The removal efficiency on regenerated MgAl-TA adsorbent are shown in Fig. 9. The percentages of adsorption of Cu^{2+} were found to be 94.43, 88.18, 84.46, 80.01, and 76.74%, respectively, for the as-prepared, 1st, 2nd, 3rd, and 4th regenerated adsorbent, showing the better re-use performance of MgAl-TA adsorbent. Fig. 10 shows the XRD patterns of the as-prepared, 1st and 4th regenerated MgAl-TA LDH adsorbents. It is found that after regeneration the adsorbent still keep the LDH structure. However, the (0 0 3) diffraction peak moves to higher diffraction angle, showing the decrease in the interlayer space. This result suggests that the decrease in amount of TA ions in the interlayer space, resulting in the decrease in removal efficiency.

4. Conclusions

The adsorption of Cu^{2+} on adsorption of Cu was studied, and some influence factors such as contact time, initial Cu^{2+} concentration, adsorbent dosage, solution pH, and adsorption temperature were investigated. It was shown that Cu^{2+} could be rapidly adsorbed to the equilibrium values within 60 min. The removal efficiency increased, but the amount of Cu^{2+} adsorbed on unit weight adsorbent decreased, with the increase in MgAl-TA LDH dosage. The suitable MgAl-TA LDH adsorbent may be about 4 g L^{-1}. The higher in the initial Cu^{2+} concentration, the lower in removal

efficiency, but the higher in per mass adsorbed amount, showing the adsorbent had the capacity for removal of Cu^{2+} with higher concentration. The initial solution pH had a strong influence on Cu^{2+} adsorption, the removal efficiency increased with the increase in pH values and then reduced to a plateau, the suitable pH value is about 5–6. The adsorption isotherms data were fitted by Langmuir isotherms, predicting the adsorption of Cu^{2+} on MgAl-TA LDH adsorbents was a monolayer adsorption. The adsorption kinetics data were well described by a pseudo-second order kinetic model, showing the adsorption process was controlled by chemical process, but the intra-particle diffusion could not be ignored. The results of adsorption thermodynamic suggested that the interaction of Cu^{2+} adsorbed by MgAl-TA adsorbents was spontaneous and endothermic. Moreover, the regeneration ability investigation results showed that after regeneration the MgAl-TA LDH structure could be reconstructed, keeping a higher removal efficiency as that of the as-prepared MgAl-TA LDH adsorbent.

References

[1] M. Hua, S. Zhang, B. Pan, W. Zhang, L. Lv, Q. Zhang, Heavy metal removal from water/wastewater by nanosized metal oxides: A review, J. Hazard. Mater. 212 (2012) 317–331.

[2] M. Jian, C. Tang, M. Liu, Adsorptive removal of Cu^{2+} from aqueous solution using aerobic granular sludge, Desalin. Water Treat. 52 (2014) 1–10, in press. doi: 10.1080/19443994.2014.895782.

[3] F. Fu, Q. Wang, Removal of heavy metal ions from wastewaters: A review, J. Environ. Manage. 92 (2011) 407–418.

[4] M. Hossain, H. Ngo, W. Guo, T. Nguyen, S. Vigneswaran, Performance of cabbage and cauliflower wastes for heavy metals removal, Desalin. Water Treat. 52 (2014) 844–860.

[5] C. Saka, Ö. Şahin, M.M. Küçük, Applications on agricultural and forest waste adsorbents for the removal of lead (II) from contaminated waters, Int. J. Environ. Sci. Technol. 9 (2012) 379–394.

[6] W. Wan Ngah, M.A.K.M. Hanafiah, Removal of heavy metal ions from wastewater by chemically modified plant wastes as adsorbents: A review, Bioresour Technol. 99 (2008) 3935–3948.

[7] S.S. Ibrahim, H.S. Ibrahim, N.S. Ammar, H.H. Abdel Ghafar, Applicability of Egyptian diatomite for uptake of heavy metals, Desalin. Water Treat. 51 (2013) 2343–2350.

[8] X. Qiu, K. Sasaki, T. Hirajima, K. Ideta, J. Miyawaki, One-step synthesis of layered double hydroxide-intercalated gluconate for removal of borate, Sep. Purif. Technol. 123 (2014) 114–123.

[9] J.-Q. Jiang, S.M. Ashekuzzaman, Development of novel inorganic adsorbent for water treatment, Curr. Opin. Chem. Eng. 1 (2012) 191–199.

[10] D. Zhao, G. Sheng, J. Hu, C. Chen, X. Wang, The adsorption of Pb(II) on Mg_2Al layered double hydroxide, Chem. Eng. J. 171 (2011) 167–174.

[11] M. Park, C.L. Choi, Y.J. Seo, S.K. Yeo, J. Choi, S. Komarneni, J.H. Lee, Reactions of Cu^{2+} and Pb^{2+} with Mg/Al layered double hydroxide, Appl. Surf. Sci. 37 (2007) 143–148.

[12] R. Rojas, Copper, lead and cadmium removal by Ca Al layered double hydroxides, Appl. Surf. Sci. 87 (2014) 254–259.

[13] J. Pérez-Esteban, C. Escolástico, A. Moliner, A. Masaguer, Chemical speciation and mobilization of copper and zinc in naturally contaminated mine soils with citric and tartaric acids, Chemosphere 90 (2013) 276–283.

[14] T. Kameda, S. Saito, Y. Umetsu, Mg–Al layered double hydroxide intercalated with ethylene-diaminetetraacetate anion: Synthesis and application to the uptake of heavy metal ions from an aqueous solution, Sep. Purif. Technol. 47 (2005) 20–26.

[15] M.R. Pérez, I. Pavlovic, C. Barriga, J. Cornejo, M.C. Hermosín, M.A. Ulibarri, Uptake of Cu^{2+}, Cd^{2+} and Pb^{2+} on Zn–Al layered double hydroxide intercalated with edta, Appl. Surf. Sci. 32 (2006) 245–251.

[16] T. Kameda, H. Takeuchi, T. Yoshioka, Uptake of heavy metal ions from aqueous solution using Mg–Al layered double hydroxides intercalated with citrate, malate, and tartrate, Sep. Purif. Technol. 62 (2008) 330–336.

[17] Y. Feng, H. Zhou, G. Liu, J. Qiao, J. Wang, H. Lu, L. Yang, Y. Wu, Methylene blue adsorption onto swede rape straw (*Brassica napus* L.) modified by tartaric acid: Equilibrium, kinetic and adsorption mechanisms, Bioresour Technol. 125 (2012) 138–144.

[18] T. Kameda, H. Takeuchi, T. Yoshioka, Hybrid inorganic/organic composites of Mg–Al layered double hydroxides intercalated with citrate, malate, and tartrate prepared by co-precipitation, Mater. Res. Bull. 44 (2009) 840–845.

[19] S.J. Santosa, E.S. Kunarti, Synthesis and utilization of Mg/Al hydrotalcite for removing dissolved humic acid, Appl. Surf. Sci. 254 (2008) 7612–7617.

[20] F. Jiao, H. Song, W. Yang, X. Jiang, X. Chen, J. Yu, Enantioselective separation of tryptophan by Mg–Al layered double hydroxides intercalated with tartaric acid derivative, Appl. Surf. Sci. 75 (2013) 92–99.

[21] Y. Liu, M. Chen, H. Yongmei, Study on the adsorption of Cu(II) by EDTA functionalized Fe_3O_4 magnetic nano-particles, Chem. Eng. J. 218 (2013) 46–54.

[22] H. Znad, Z. Frangeskides, Chicken drumstick bones as an efficient biosorbent for copper (II) removal from aqueous solution, Desalin. Water Treat. 52 (2013) 1560–1570.

[23] S. Swain, T. Patnaik, V. Singh, U. Jha, R. Patel, R. Dey, Kinetics, equilibrium and thermodynamic aspects of removal of fluoride from drinking water using mesostructured zirconium phosphate, Chem. Eng. J. 171 (2011) 1218–1226.

[24] A.A. Khan, R.P. Singh, Adsorption thermodynamics of carbofuran on Sn (IV) arsenosilicate in H^+, Na^+ and Ca^{2+} forms, Colloid Surf. 24 (1987) 33–42.

[25] T. Qiu, Y. Zeng, C. Ye, H. Tian, Adsorption thermodynamics and kinetics of p-xylene on activated carbon, J. Chem. Eng. Data 57 (2012) 1551–1556.

[26] W. Zou, R. Han, Z. Chen, Z. Jinghua, J. Shi, Kinetic study of adsorption of Cu(II) and Pb(II) from aqueous solutions using manganese oxide coated zeolite in batch mode, Colloid Surf., A 279 (2006) 238–246.